COMPARATIVE STUDY OF DIFFERENT CONTROL STRATEGIES IN THE CERAMIC TILE FORMING STAGE

J. Boix [1], G. Mallol [1], D. Llorens [1], M.J. Sánchez [1],

D. Santos [2], D. Hotza [2]

[1] Instituto de Tecnología Cerámica (ITC). Asociación de Investigación de las Industrias Cerámicas (AICE), Universitat Jaume I. Castellón. Spain

[2] Universidade Federal de Santa Catarina, Department of Mechanical Engineering, Florianópolis, SC. Brazil

ABSTRACT

This study presents an industrially validated model that relates the main control variables of the ceramic tile manufacturing process stages to their interactions with tile properties, which enables tile end size to be predicted. The validated model is used to analyse the different control strategies that can be applied in the porcelain tile forming stage, as well as their influence on the dimensional stability of the end product.

1. INTRODUCTION

At present, the demanding dimensional tolerances imposed by the market on the end product require thorough control of all the ceramic tile manufacturing process stages. However, the current state of the technology does not allow all tile sizes to be kept within the tolerance ranges used, in particular when large-sized products (larger than 500 mm) are involved.

Previous research studies [1], [2] showed that lack of dimensional stability in ceramic tile bodies was due to improper performance of the pressing and/or firing operations. In the case of porcelain tiles, calibres are fundamentally due to variations in the average dry bulk density between unfired tile bodies, as these differences cannot be corrected during firing.

The flow chart in Figure 1 schematically illustrates the different dimensional changes that ceramic tile bodies undergo during the manufacturing process, and the different process variables associated with those changes.

The subscripts of each variable represent, in sequential form, the related unit operations. The variables shown above the arrows in the flow chart are the variables that are known to be independent, their values being determined by the processing conditions. The variables shown below the arrows are the dependent variables, whose values may be estimated from the independent variables.

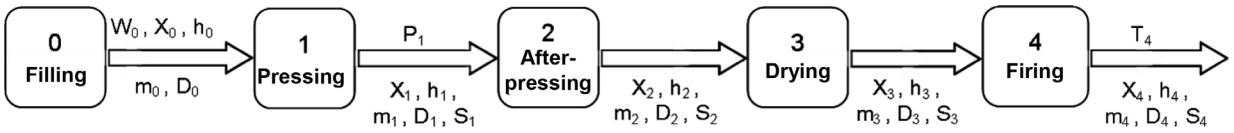

Figure 1. Flow chart and ceramic tile manufacturing process variables.

Stage 0 corresponds to press die filling. In this stage, the dimensions (thickness, h, and size, X) refer to the press die volume (h_0 and X_0). In stage 1, pressing, the spray-dried powder is compacted, powder bed volume decreases, and the dimensions of the tile body correspond to h_1 and X_1, where $X_1=X_0$. After pressing, stage 2, the tile expands, known as after-pressing expansion. Finally, in stages 3 and 4, tile drying and firing shrinkage take place, respectively. The following variables are identified in the diagram in Figure 1:

W_0: Spray-dried powder moisture content (%)

X_i: Size (mm)

h_i: Thickness (mm)

m_i: Mass (kg)

D_i: Density (kg/m^3)

P_1: Maximum pressing pressure (MPa)

S_i: Linear dimensional change (%)

T_4: Peak firing temperature (°C)

To determine tile end size, X_4, the variables S_2, S_3, and S_4, corresponding to the dimensional changes that take place in the tile, must be taken into account. These variables are calculated as a percentage, in the form:

Eq. 1 $$Si = 100\ (X_{i-1}-X_i)/X_{i-1}$$

Where 'i' is the subscript corresponding to each stage. Applying Eq. 1 to the different process stages and taking into account that $X_0 = X_1$ yields Eq. 2, which relates tile end size to the size of the die cavity:

Eq. 2 $$X_4 = (100-S_2)\ (100-S_3)\ (100-S_4)\cdot 10^{-6} X_1$$

For a given composition, after-pressing expansion (S_2) and drying shrinkage (S_3) basically depend on powder moisture content (W_0) and maximum pressing pressure (P_1). In turn, firing shrinkage (S_4) is a function mainly of peak firing temperature (T_4) and of density on a dry basis (D_3), this last variable depending on W_0 and P_1. Therefore, the different dimensional changes undergone by tile bodies, as well as their dry bulk density, may be calculated from the independent variables W_0, P_1, and T_4, [3], using Eqs. 3 to 6.

Eq. 3 $$S_2 = f\ (W_0, P_1)$$

Eq. 4 $$S_3 = f\ (W_0, P_1)$$

Eq. 5 $$S_4 = f\ (D_3, T_4)$$

Eq. 6 $$D_3 = f\ (W_0, P_1)$$

Eq. 2 and Eqs. 3 to 6 allow the end size of the tile body to be estimated as a function of the independent variables. Similar expressions could be defined to calculate the end thickness of the fired tile and/or of the body during the different process stages. In this case, the linear dimensional changes (S_i) in the tile sizes should be replaced with the dimensional changes in tile thickness. Indeed, in experimental studies currently in course, it has been verified that the dimensional changes undergone by the product during the process and, in particular, during the expansion stage that takes place immediately after pressing, differ significantly. Consequently, the changes that tile bodies proportionally undergo in their side dimensions cannot be assumed to be the same as those that they undergo in thickness. In any event, as ceramic tile thickness is a variable that is not terribly important from a process control standpoint, the present paper only examines the control actions aimed at keeping fired tile end size constant.

2. OBJECTIVES

The objectives of the present study were as follows:

- To obtain a mathematical model, validated on an industrial scale for a porcelain tile composition, which allows the end dimensions of the ceramic tiles to be estimated.

- Using the previously validated model, to compare the effect of different possible control strategies in the tile body forming stage on end product dimensional stability.

3. MATERIALS AND METHODOLOGY

The study was carried out using a standard spray-dried powder composition for porcelain tile manufacture. Experiments were conducted, first, on a laboratory scale with a view to finding the regression equations that related dry bulk density (D_3), after-pressing expansion (S_2), drying shrinkage (S_3) and firing shrinkage (S_4) of the composition to the independent variables W_0, P_1 and T_4 .

The samples were prepared by conditioning the press powder at different moisture contents and subsequently pressing cylindrical test pieces at four maximum pressures, using a cylindrical die, 40 mm in diameter. After the pieces had been pressed, their after-pressing expansion (S_2) was determined, and they were dried in a laboratory oven for at least 2 hours at 110ºC. After drying, test piece drying shrinkage S_3) and dry bulk density (D_3) were determined. They were then fired in an electric laboratory kiln, at four peak firing temperatures, and their firing shrinkage (S_4) and external porosity, as water absorption capacity, were determined. The processing conditions used in the experiments were selected such that they encompassed the usual working range of the selected composition.

In order to validate the equations in the model in industrial practice, a series of industrial trials were conducted in a ceramic tile manufacturing line using the same working composition. The trials consisted of pressing bodies with a nominal fired size of 700 mm x 450 mm in an industrial hydraulic press at three different maximum pressing pressures and at a moisture content of about 6.1%. The die used in the operations had four cavities with internal dimensions of 754 mm x 503 mm. After the bodies had been formed, they were dried in an industrial vertical dryer and fired in a single-deck roller kiln at a peak temperature of 1200ºC. The dimensions of the different test bodies were determined after drying and after firing. Their green and dry bulk density was similarly determined, using the mercury displacement method.

4. EXPERIMENTAL RESULTS

4.1. OBTAINMENT OF THE CONSTITUTIVE EQUATIONS AT LABORATORY LEVEL

This section sets out the equations that explain the behaviour of the bodies, the equations being obtained in accordance with the methodology described in the previous section.

- After-pressing expansion:

Eq. 7 $$-S_2 = (4.0 \cdot 10^{-4} P_1 - 0.04)\, W_0 + 4.93 \cdot 10^{-3}\, P_1 + 1.24$$

- Drying shrinkage:

At laboratory level, the contribution of the drying shrinkage, S_3, could not be determined from the measurement of the dimensions of the test pieces, owing to the small magnitude of this variable.

- Compaction diagram:

Eq. 8 $$D_3 = 174.9\, W_0^{-0.13} \cdot \ln P_1 + 1219.2\, W_0^{0.10}$$

- Linear firing shrinkage:

Eq. 9 $$S_4 = (3.94 \cdot 10^{-7}\, T_4^2 - 1.08 \cdot 10^{-3}\, T_4 + 0.71)\, D_3 - 1.45 \cdot 10^{-3}\, T_4^2 + 3.71\, T_4 - 2334.5$$

4.2. VALIDATION OF THE MODEL ON AN INDUSTRIAL SCALE

The average values of the different variables determined in the manufacturing line are detailed in Table 1, in accordance with the nomenclature used in Figure 1. As a rectangular size was used, the values corresponding to test piece size distinguish between length(Xli) and width (Xwi).

FILLING			PRESSING	AFTER-PRESSING	DRYING			FIRING	
W_0 (%dry basis)	Xl_0 (mm)	Xw_0 (mm)	P_1 (MPa)	D_2 (kg/m³)	D_3 (kg/m³)	Xl_3 (mm)	Xw_3 (mm)	Xl_4 (mm)	Xw_4 (mm)
6.1	754	503	33.8	2060	1955	761.8	508.2	704.6	470.1
6.1	754	503	38.5	2076	1972	761.6	508.1	707.0	471.7
6.1	754	503	44.2	2094	1990	761.9	508.3	708.5	472.8

Table 1. Process data obtained under industrial conditions for the validation of the constitutive model.

4.2.1. Estimation of after-pressing expansion (S_2) and drying shrinkage (S_3) under industrial conditions

During the performance of the industrial trials, the high brittleness of the unfired bodies prevented their dimensions from being determined. Consequently, no experimental data were available to directly calculate the after-pressing expansion and drying shrinkage under industrial conditions.

It had been assumed, a priori, based on the laboratory data that had shown that the drying shrinkage of the working composition was practically negligible, that the dimensional changes in the tile bodies during industrial drying would also be very small. Therefore, to evaluate the resulting precision in the estimation of tile size when the tiles exited the dryer(X_3), only considering the after-pressing expansion, the variation with pressure of the percentage expansion that the bodies would undergo according to the laboratory model and the variation of expansion that really took place at industrial level, according to Eq. 10, have been plotted in Figure 2.

Eq. 10 $$S_2 = 100\ (X_0-X_3)/X_0$$

As may be observed, although the industrial expansion values followed the trend marked by Eq. 7, they lay slightly above the values estimated under laboratory conditions. This indicated that the assumption made was not applicable and the dimensional change relating to drying shrinkage under industrial conditions could not be considered negligible. Consequently, the average industrial drying shrinkage would be 0.25%, a value corresponding to the average difference between the after-pressing expansion values calculated from Eq. 7 and those obtained from Eq. 10.

Eq. 11 $$D_3 = \frac{D_2}{1+\frac{W_0}{100}}$$

D_3 (kg/m³)	$D_{3\ calculated}$ (kg/m³)	ΔD_3 (kg/m³)
1954	1942	12
1972	1957	15
1990	1974	16

Table 2. Experimental data and values calculated from Eq. 11 of bulk density.

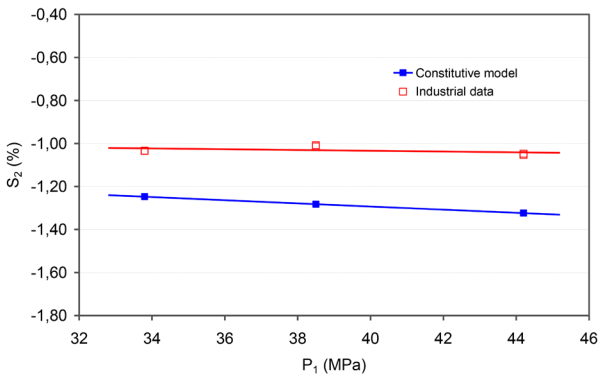

Figure 2. Variation of after-pressing expansion with pressure under industrial and under laboratory conditions.

Despite the small magnitude of drying shrinkage at industrial level, its importance was also reflected in the industrially obtained wet and dry bulk density values.

Indeed, if the dry bulk densities (D_3) are calculated from the wet bulk density values (D_2) (see Table 1), just considering the mass loss related to drying (Eq. 11), it may be observed that there was a significant discrepancy with relation to the experimentally measured values.

This observation revealed that tile body drying took place with a non-negligible dimensional change, so that Eq. 11 was not valid and needed to be replaced with Eq. 12, which took into consideration tile volume change (V_i) during drying.

Eq. 12
$$D_3 = \frac{D_2}{1+\frac{W_0}{100}}\frac{V_2}{V_3}$$

Eq. 13
$$S_3^V = 100\ (V_2 - V_3)/V_2$$

Eq. 14
$$S_3^V = 3\ S_3$$

Eq. 15
$$s_3 = \frac{100}{3}\left(1-\frac{D_2}{D_3}\frac{100}{100+W_0}\right)$$

Assuming that the drying shrinkage of the bodies took place isotropically, the relationship between linear drying shrinkage (S_3) and volumetric drying shrinkage (S_3^V) (Eq. 13) could be calculated by means of Eq. 14.

Thus, combining Eqs. 12, 13, and 14 enabled an expression to be obtained (Eq. 15) that allowed the drying shrinkage of the tile bodies to be calculated from their dry and wet bulk densities.

A comparison is shown in Table 3, for each pressing condition, of the drying shrinkage values calculated from Eq. 15, and the values obtained from the industrial data of X_3, assuming that the after-pressing expansion of the bodies can be estimated from Eq. 7.

As may be observed, there was little difference between the calculated drying shrinkages using the two methods. This confirms, on the one hand, that industrial drying shrinkage was not negligible and may be deemed isotropic and, on the other, that the after-pressing expansion estimated with the model correctly reproduced tile body behaviour under industrial conditions.

P_1 (MPa)	$S_{3\ (Ec.\ 15)}$ (%)	$S_{3\ (Ec.\ 7\ y\ X3)}$ (%)
33.8	0.21	0.21
38.5	0.26	0.27
44.2	0.27	0.28
Average	0.25	0.25

Table 3. Dying shrinkage calculated with the body densities, considering the laboratory after-pressing expansion.

4.2.2. Estimation of dry bulk density (D_3) from the compaction diagram

To validate the equation of the compaction diagram (Eq. 8), the variation of dry bulk density has been plotted as a function of maximum pressing pressure under industrial and under laboratory conditions in Figure 3. As may be observed, at all pressures, the dry bulk density of the bodies formed under industrial conditions was always slightly higher than that estimated from the laboratory diagram. This could be due to a mismatch between the pressure values provided by the pressure transducers of the presses used in the work and/or to differences in the pressing cycles used, for example in the maximum pressure application time. In any event, it is interesting to note that the differences

observed were very insignificant, as they only involved an error of 0.3% in relation to the estimated industrial bulk density.

Additional studies [4] have shown that, in the usual working ranges, the differences observed in bulk density were independent of pressure and moisture content and were constant in time, unless there was a significant change in spray-dried powder composition. Consequently, the laboratory compaction diagram could be adapted to the industrial conditions by introducing an independent term in Eq. 8.

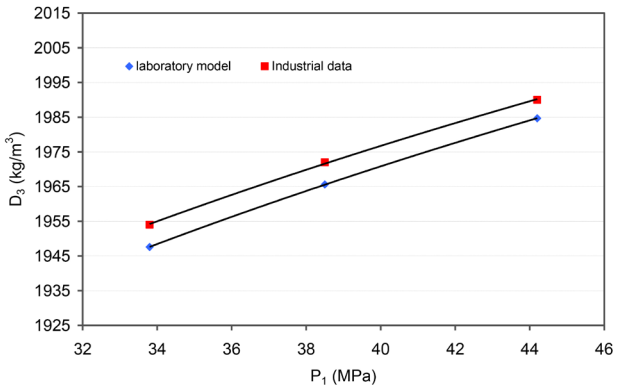

Figure 3. Variation of dry bulk density with pressing pressure under industrial and under laboratory conditions.

The industrial diagram thus adopted the form of Eq. 16 in which, for the entire range of working pressures, the independent term represented the average difference of 6 kg/m^3 observed between the industrial bulk density and the bulk density estimated from the model.

Eq. 16

$$D_3 = 174{,}9\ W0^{-0{,}13} \cdot \ln P_1 + 1219{,}2\ W_0^{0{,}10} + 6$$

4.2.3. Estimation of firing shrinkage (S_4) from the vitrification diagram

The variation of firing shrinkage as a function of bulk density under industrial conditions and under laboratory conditions, for the firing temperature used in the industrial trials, has been plotted in Figure 4. As may be observed, at any bulk density, the shrinkage of the industrial bodies was always slightly higher than the estimated shrinkage, the difference being constant and very small (0.2%) within the range of studied bulk densities. This small difference might be caused by the scale-up from laboratory conditions (in which small electric kilns were used) to industrial conditions, where firing took place continuously in large single-deck kilns with a great number of natural gas burners.

Complementary studies [4] have shown that the observed differences were independent of the firing temperature and dry bulk density. Therefore, the laboratory vitrification diagram could be extrapolated to industrial conditions by introducing a new independent term, thus enabling the shrinkage of the industrial tile bodies to be calculated from Eq. 17.

Eq. 17 $$S_4 = (3.94 \cdot 10^{-7}\ T_4^2 - 1.08 \cdot 10^{-3}\ T_4 + 0.71)\ D_3 - 1.45 \cdot 10^{-3}\ T_4^2 + 3.71\ T_4 - 2334.3$$

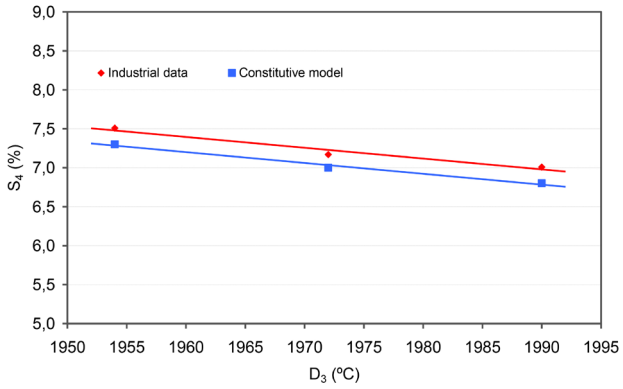

Figure 4. Variation of firing shrinkage with bulk density under industrial and under laboratory conditions.

4.2.4. Estimation of tile body end size (X_4) from the model

Once the different equations making up the constitutive model had been validated, it was possible to determine the fired body end size using Eq. 2. In view of the difficulty of performing industrial trials that would enable the relationship between drying shrinkage and P_1 and W_0 to be obtained, this was assumed to have a constant value of 0.25%. The other dimensional changes, S_2 and S_4, were calculated from Eqs. 7 and 17, respectively, the values of Xl_4 being obtained that are detailed in Table 4. It may be observed that the sizes estimated with the validated model were very close to the experimental values obtained under industrial conditions, despite assuming drying shrinkage to be constant. Indeed, the maximum error in the estimation was only ±0.2 mm.

	Width			Length		
P_1 (MPa)	Xw_4 (mm)	$Xw_{4\ calculada}$ (mm)	ΔXw_4 (mm)	Xl_4 (mm)	$Xl_{4\ calculada}$ (mm)	ΔXl_4 (mm)
33.8	470.1	469.9	-0.2	704.6	704.4	-0.2
38.5	471.7	471.7	0.0	707.0	707.1	0.1
44.2	472.8	472.9	0.1	708.5	708.7	0.2

Table 4. Estimation of industrial tile end size using the validated model.

4.3. COMPARATIVE ANALYSIS OF DIFFERENT CONTROL STRATEGIES

In industrial practice, with a view to keeping tile end size within certain maximum margins of variation, the pressing conditions are modified to offset fluctuations in spray-dried powder moisture content. Using the validated model, it was possible to simulate tile body behaviour for the work composition, considering three different control scenarios:

- Control based on wet bulk density: this consists of modifying the maximum pressing pressure to keep wet bulk density constant in the freshly pressed bodies.

- Control based on dry bulk density: this consists of modifying the maximum pressing pressure to keep dry bulk density constant in the bodies.

- No control: this would involve not modifying the pressure, independently of the fluctuations in spray-dried powder moisture content.

In industrial practice, pressing control is usually based on the wet bulk density of the tile bodies. However, recent years have witnessed the spread of an automatic control system, based on keeping dry bulk density constant, which allows the maximum pressing pressure to be modified by continuously measuring the spray-dried powder moisture content and estimating tile body density from the compaction diagram.

The plot in Figure 5 shows, for each of the studied control strategies, the variation of tile body end size with spray-dried powder moisture content, within the usual range of variation in moisture content under industrial conditions. In each case, the settings of the control variable were chosen such that, for a moisture content of 6%, a tile end size of about 700 mm was obtained.

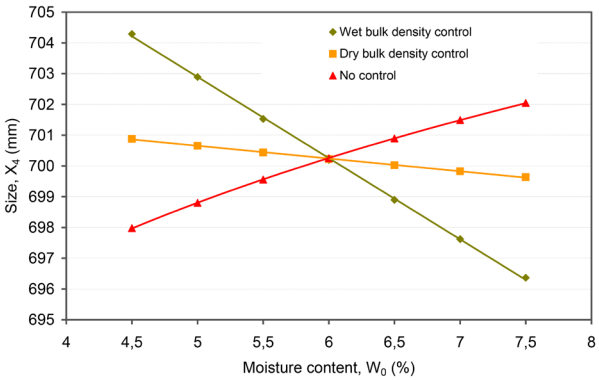

Figure 5. Variation of tile body end size with moisture content for three different control strategies.

Table 5 details, for each of the simulated strategies, the values of the control variables, the absolute value of parameter $\Delta X_4/\Delta W_0$ corresponding to the slope of the curves plotted in Figure 5, and the number of calibres that would be obtained in a production batch that exhibited a maximum variation in moisture content of 1% during tile forming, for a calibre tolerance of 1 mm.

Control strategy	P_1 (MPa)	D_2 (kg/m^3)	D_3 (kg/m^3)	$\lvert\Delta X_4/\Delta W_0\rvert$ (mm/%)	Number of calibres
Wet bulk density control	Variable	2030	Variable	2.6	3
Dry bulk density control	Variable	Variable	1930	0.4	1
No control	28.9	Variable	Variable	1.3	2

Table 5. Operating variables and dimensional changes undergone by the tile bodies in the production process for the three studied control strategies.

As may be observed, the control strategy based on keeping wet bulk density constant generated the greatest variation in tile end size, for a certain change in spray-dried powder moisture content. In fact, from the viewpoint of end product dimensional stability, this was even less effective than no control. That is, under industrial conditions, it was preferable to work at constant pressure, independently of the variations in moisture content of the spray-dried powder, rather than attempt to keep the wet bulk density constant in the tile bodies. Indeed, for a variation in moisture content of 1%, control based on wet bulk density would provide a size variation of 2.6 mm, whereas the absence of any type of control would only generate a size variation of 1.3 mm.

In the studied cases, these two strategies were much less effective than control based on keeping dry bulk density constant in the tile bodies, as this approach only led to a dimensional change of 0.4 mm at a variation in moisture content of 1%.

In addition, the data in Table 5 indicate that a batch produced with a variation of 1% in spray-dried powder moisture content, controlled by measuring wet bulk density, would exhibit at least 3 calibres, whereas the same batch, produced without any control, would exhibit only 2 calibres. However, if control had been based on measuring dry bulk density, the batch would have exhibited just one calibre in sorting.

In previous studies [5], dry bulk density control was put forward as the most appropriate control strategy to keep fired tile end size constant. Although the simulations performed confirmed that this control strategy was much more satisfactory than no control or wet bulk density control, they also revealed that there was always a slight variation in the end size with spray-dried powder moisture content, despite keeping dry bulk density constant in the bodies.

This was due to the dependence on moisture content and pressure that both after-pressing expansion and drying shrinkage of the bodies exhibited. Indeed, to keep tile bulk density steady, it is essential to modify the pressing pressure, which originates non-negligible changes in after-pressing expansion and drying shrinkage, which in turn lead to changes in tile end size. In particular, according to the data in Table 5, for the working composition, a change in moisture content of 1% would produce a change in tile end dimensions of 0.4 mm, accounting for 40% of the maximum allowable size variation for a calibre tolerance of 1 mm.

Given the demanding dimensional tolerances that prevail for this type of product, the results obtained in the simulations highlight the interest of considering a new pressing control strategy. This new strategy, unlike current control based on iso-compaction diagrams, would be based on a hypothetical iso-size diagram, from which the pressing conditions would be fixed for obtaining the same tile end size, and not on a constant dry bulk density. In fact, as may be observed in the plot in Figure 6, in such a control strategy, the bulk density setting would need to be modified as a function of the evolution of spray-dried powder moisture content to offset the variations caused by after-pressing expansion and drying shrinkage.

In particular, the results of the simulations shown in Figure 6 indicate that, for control by iso-size, a 1.5% increase in spray-dried powder moisture content would require increasing the bulk density setting by 5 kg/m^3, so that the required decrease in pressure would be less significant than in the dry bulk density-based control. This approach would offset the change in after-pressing expansion, which would assure consistent tile body end size.

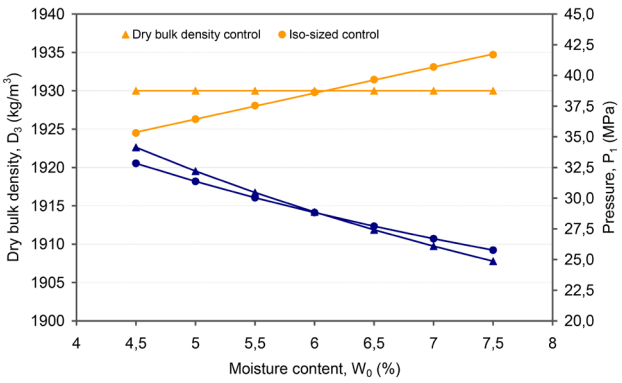

Figure 6. Variation of dry bulk density and end size as a function of moisture content for hypothetical control based on an iso-size diagram.

5. CONCLUSIONS

- A constitutive model, validated on an industrial scale, allows the end size of ceramic tile bodies to be precisely estimated for given operating conditions and spray-dried powder characteristics.

- The simulation of different control scenarios reveals that control based on dry bulk density is much more effective than the traditional control strategy based on measuring wet bulk density of the tile bodies.

- Control of the pressing stage based on measuring wet bulk density is not very effective for controlling dimensional stability, as it generates a greater variation in tile end size than no control.

- To improve the current state-of-the-art it is essential to consider the effect of after-pressing expansion and drying shrinkage on the dimensional stability of the end product. This opens up avenues to pressing control based on iso-size diagrams.

REFERENCES

[1] AMORÓS, J.L. Pastas cerámicas para pavimentos de monococción: Influencia de las variables de prensado sobre las propiedades de la pieza en crudo y sobre su comportamiento durante el prensado y la cocción. Valencia University. 1987, p.61 [Doctoral dissertation]

[2] AMORÓS, J.L. et al. Mejora de la estabilidad dimensional de piezas de gres porcelánico a través de la medida en continuo de la humedad de los soportes prensados. Castellón. Qualicer 2004.

[3] SANTOS B., D. Controle do tamanho final de porcelanatos: modelagem e simulaçao das etapas de prensagem e secagem. Florianópolis, SC: Universidade Federal de Santa Catarina. 2011 [Doctoral dissertation]

[4] POYATOS, A. et al. Nuevo sistema y metodología para la eliminación de los calibres en el proceso de fabricación de baldosas cerámicas. Bol. Soc. Esp. Ceram. Vidrio. 49(2), 147-151, 2010

[5] MALLOL, G., Control y automatización en la industria cerámica. Evolución y perspectivas. Castellón. Qualicer 2006.